Clinical Cancer Research

Clinical Efficacy and Tumor Microenvironment Influence in a Dose-Escalation Study of Anti-CD19 Chimeric Antigen Receptor T Cells in Refractory B-Cell Non-Hodgkin's Lymphoma

Zi-Xun Yan[1], Li Li[1], Wen Wang[2], Bin-Shen OuYang[3], Shu Cheng[1], Li Wang[1,4], Wen Wu[1], Peng-Peng Xu[1], Muharrem Muftuoglu[5], Ming Hao[2], Su Yang[2], Mu-Chen Zhang[1], Zhong Zheng[1], James Li[2], and Wei-Li Zhao[1,4]

Abstract

Purpose: Anti-CD19 chimeric antigen receptor (CAR) T cells represent a novel immunotherapy and are highly effective in treating relapsed/refractory B-cell non-Hodgkin's lymphoma (B-NHL). How tumor microenvironment influences clinical response to CAR T therapy remains of great interest.

Patients and Methods: A phase I, first-in-human, dose-escalation study of anti-CD19 JWCAR029 was conducted in refractory B-NHL (NCT03355859) and 10 patients received CAR T cells at an escalating dose of 2.5×10^7 ($n = 3$), 5×10^7 ($n = 4$), and 1×10^8 ($n = 3$) cells. Core needle biopsy was performed on tumor samples collected from diffuse large B-cell lymphoma patients on Day −6 (1 day before lymphodepletion) and on Day 11 after CAR T-cell infusion when adequate CAR T-cell expansion was detected.

Results: The overall response rate was 100%, with 6 of 9 (66.7%) evaluable patients achieving complete remission. The most common adverse events of grade 3 or higher were neutropenia (10/10, 100%), anemia (3/10, 30%), thrombocytopenia (3/10, 30%), and hypofibrinogenemia (2/10, 20%). Grade 1 cytokine release syndrome occurred in all patients and grade 3 neurotoxicity in 1 patient. The average peak levels of peripheral blood CAR T cells and cytokines were similar in 3 different dose levels, but CAR T cells were significantly higher in patients achieved complete remission on Day 29. Meanwhile, RNA sequencing identified gene expression signatures differentially enriched in complete and partial remission patients. Increased tumor-associated macrophage infiltration was negatively associated with remission status.

Conclusions: JWCAR029 was effective and safe in treating refractory B-NHL. The composition of the tumor microenvironment has a potential impact in CAR T therapy response.

Introduction

B-cell non-Hodgkin's lymphoma (B-NHL) represent the most common lymphoid malignancies. Although the anti-CD20 antibody rituximab combined with chemotherapy significantly improves the clinical outcome of B-NHL, the prognosis is extremely poor in patients who are resistant to primary or salvage immunochemotherapy or in patients who encounter a relapse after hematopoietic stem-cell transplantation (HSCT; ref. 1). Anti-CD19 chimeric antigen receptor (CAR) T cells induce high response rates and may be potentially curative in relapsed or refractory B-NHL. A phase I to II study of axicabtagene ciloleucel with a CD28 costimulatory domain in refractory B-NHL (ZUMA-1) demonstrated the best overall response rate (ORR) at 82%, with 58% of patients meeting criteria for complete remission (CR) at a dose of 2×10^6 CAR+ cells/kg (2). For a flat dose, the best ORR and CR rate of tisagenlecleucel with a 4-1BB costimulatory domain were 52% and 40%, respectively, at a median dose of 3×10^8 CAR+ cells in relapsed or refractory diffuse large B-cell lymphoma (DLBCL; JULIET; ref. 3). Lisocabtagene maraleucel (JCAR017) is another 4-1BB CAR T product formulated at a specified CD4:CD8 composition. A phase I study of JCAR017 (TRANSCEND NHL-001) achieved the best ORR and CR rate at 81% and 63%, respectively, with 1×10^8 CAR+ cells in relapsed or refractory B-NHL (4). However, it remains greatly challenging to predict clinical efficacy for patients who receive CAR T therapy.

Resistance to CAR T cells is multifactorial, including antigen escape through acquired mutation and alternative splicing of CD19, masking of antigenic epitope by anti-CD19 CARs, and failure of CAR T cells to persist *in vivo* (5–8). More recently, the inability of CAR T cells to proliferate in tumor sites has emerged as an important issue impacting the clinical response of CAR T therapy (9). Tumor-driven immunosuppressive

[1]State Key Laboratory of Medical Genomics, Shanghai Institute of Hematology, Shanghai Rui Jin Hospital, Shanghai Jiao Tong University School of Medicine, Shanghai, China. [2]JW Therapeutics, Shanghai, China. [3]Department of Pathology, Shanghai Rui Jin Hospital, Shanghai Jiao Tong University School of Medicine, Shanghai, China. [4]Pôle de Recherches Sino-Français en Science du Vivant et Génomique, Laboratory of Molecular Pathology, Shanghai, China. [5]Department of Leukemia, University of Texas - MD Anderson Cancer Center, Houston, Texas.

Note: Supplementary data for this article are available at Clinical Cancer Research Online (http://clincancerres.aacrjournals.org/).

Z.-X. Yan, L. Li, W. Wang, and B.-S. OuYang contributed equally to this article.

Corresponding Author: Wei-Li Zhao, State Key Laboratory of Medical Genomics, Shanghai Institute of Hematology, Shanghai RuiJin Hospital, Shanghai Jiao Tong University School of Medicine, 197 Rui Jin Er Road, Shanghai 200025, China. Phone: 86-21-64370045; Fax: 86-21-64743206; E-mail: zhao.weili@yahoo.com

Clin Cancer Res 2019;25:6995–7003

doi: 10.1158/1078-0432.CCR-19-0101

Translational Relevance

This phase I, first-in-human, dose-escalation clinical trial of anti-CD19 JWCAR029 on refractory B-NHL demonstrated that complete remission can be achieved at a low dose of CAR T cells and the tumor microenvironment has a potential impact on the clinical response of CAR T therapy. The immunosuppressive milieu of the tumor microenvironment rendered CAR T cells unable to attack the tumor and tumor-associated macrophages could serve as a predictive marker of treatment failure. Modulation of the tumor microenvironment through various strategies targeting tumor-associated macrophages and other immunosuppressive factors may be able to enhance the clinical efficacy of CAR T therapy and attain a more durable remission in B-NHL. Together, these comprehensive profiling data provide the first evidence that alterations in the tumor microenvironment are related to future mechanism-based immunotherapy.

microenvironment is found significantly associated with T-cell dysfunction induced by cytokines IL10 and TGFβ, as well as recruitment and induction of immunosuppressive cell subsets including macrophages with M2 phenotype, regulatory T (Treg) cells, myeloid-derived suppressor cells (MDSC), and other tumor-associated immune cells (10). Therefore, the role of the tumor microenvironment in response to CAR T therapy needs to be further investigated in B-NHL.

JWCAR029 engineered T cells are composed of an anti-CD19 single chain variable fragment (scFv) derived from a murine CD19-specific mAb (FMC63), CD3ζ activation domain, and 4-1BB costimulatory domain. In a phase I, first-in-human, dose-escalation study involving 10 patients with refractory B-NHL (NCT03355859), we reported the results of ORR and the primary analysis with 6 months of follow-up. Meanwhile, we evaluated the biological correlates of response and identified the influence of the tumor microenvironment, independent of the dose of CAR T cells.

Patients and Methods

Patients

This is a phase I, single-arm, open-label study evaluating the safety and efficacy of JWCAR029 in patients with relapsed or refractory CD19+ B-NHL. Eligible patients aged >18 years had histologically confirmed B-NHL (WHO 2008 classification; excluding primary central nervous system lymphoma), Eastern Cooperative Oncology Group (ECOG) <2, adequate renal, hepatic and cardiac functions, and PET-positive lesions (11). Patients were previously treated with an anti-CD20 monoclonal antibody and anthracycline-containing regimen for at least 2 cycles or experienced relapse or progression after autologous HSCT. Patients were excluded if they met one of the following criteria: history of malignancy other than non-melanoma skin carcinoma *in situ*; active hepatitis B, hepatitis C, or human immunodeficiency virus infection; pregnancy, breastfeeding, or expecting to conceive. The study was approved by the Shanghai Rui Jin Hospital Review Board with informed consent obtained in accordance with the Declaration of Helsinki.

Study design

The primary endpoints were maximum tolerated dose (MTD), adverse events (AE), and ORR. JWCAR029 was administered as a single infusion in escalating doses, beginning at 2.5×10^7 cells (dose level 1, DL1) and escalating to 5.0×10^7 cells (dose level 2, DL2) and 1.0×10^8 cells (dose level 3, DL3), according to the modified toxicity probability interval (mTPI)-2 algorithm, an interval-based Bayesian designs for dose finding (12). Dose-limiting toxicities (DLT) were defined as follows. (i) Any grade 4 or 5 AEs after infusion, excluding laboratory parameters without clinical significance. (ii) Any grade 3 AEs after infusion that did not alleviate to $\leq$ grade 2 within 7 days, excluding laboratory parameters without clinical significance. (iii) Any grade 3 epilepsy after infusion that did not alleviate to $\leq$ grade 2 in 3 days. (iv) Any $\geq$grade 3 autoimmune toxicity after infusion, excluding B-cell dysplasia. Investigators were responsible for monitoring and reporting all AEs through 24 months postinfusion. AEs were graded according to the NCI Common Terminology Criteria for Adverse Events (CTCAE), version 4.03. The cytokine release syndrome (CRS) was defined, graded, and managed according to the current concepts in the diagnosis and management of CRS (13). Tocilizumab (8 mg/kg) was used within 48 hours after patients presented with high fever (>38.6°C) and ruled out possible infection.

Secondary endpoints included pharmacokinetics, CR rate, duration of response, progression-free survival, progression-free survival ratio (previous line of treatment/JWCAR029), and overall survival.

Study procedures and treatment

Patients were enrolled following screening and confirmation of eligibility and then underwent leukapheresis to obtain peripheral blood mononuclear cells (PBMC) to manufacture the JWCAR029 cell product in a central cell processing facility. CD19-specific CAR and truncated human epidermal growth factor receptor (EGFRt) were introduced into autologous $CD4^+$ and $CD8^+$ T cells *in vitro* using a self-inactivated lentivirus vector. The final JWCAR029 cell product was washed, cryopreserved, and tested for identity, potency, sterility, and adventitious agents. After meeting acceptance criteria, the product was shipped back to the clinical sites using a validated cryo-shipper.

Lymphodepletion preconditioning was accomplished by fludarabine 25 mg/m^2/day and cyclophosphamide 250 mg/m^2/day on Day −4 to Day −2, followed by CAR T-cell infusion on Day 0. Complete blood cell count, serum biochemistry, coagulation panel, and cytokines were monitored after infusion. DLTs were evaluated from Day 1 to Day 29. Primary tumor response was assessed by PET-CT and CT on Day 29. Patients entered the follow-up phase after Day 29, and the safety, response, and persistence of JWCAR029 were evaluated at months 3, 6, 9, 12, 18, and 24. Duration of responses was assessed by CT at months 3, 6, 9, 12, 18, and 24 after a subject achieved a CR. A PET-CT was required when progression disease was suspected on follow-up phase. Disease response and duration were determined according to the "Recommendations for Initial Evaluation, Staging, and Response Assessment of Hodgkin and Non-Hodgkin Lymphoma: The Lugano Classification" (14). The pharmacokinetics study began with JWCAR029 infusion (*in vivo* amplification and persistence) until CAR T cells were no longer detected by flow cytometry or qRT-PCR.

Cytotoxic potency assay

Cytotoxic potency of JWCAR029 were analyzed with Calcein release assays. Target NALM-6 tumor cells were labeled with Calcein AM (Life Technologies; Invitrogen) for 1 hour at 37°C, and then 3,000 tumor cells were co-incubated with CAR T cells for 4 hours at effector-to-target (E:T) ratio of 20:1. Supernatants were harvested and Calcein release quantified using a BioTek Synergy 2 plate reader (Ex: 485 nm/Em: 530 nm). Cytolytic potency was calculated as % release = [(experimental release-spontaneous release)/(maximal release-spontaneous release)] × 100%, where maximal release was induced by incubation in a 1% Triton X-100 solution.

CAR T-cell detection *in vivo*

Blood samples were obtained from patients before and at predetermined intervals after CAR T cell infusion, and flow cytometry was performed to identify CD4+ and CD8+ CAR T cells as viable CD45+CD3+CD4+CD8-EGFRt+ or CD45+CD3+CD4-CD8+EGFRt+ events, respectively. EGFRt protein is co-expressed with CD19-specific CAR as a cell surface protein for analytical detection of transduced T cells. To establish loss of CAR T cell persistence due to an anti-CAR transgene immune response and to detect the integrated CAR transgene, we used quantitative RT-PCR to detect integrated transgene sequences. Forward primer: 5′-CCGTTGTCAGGCAACGTG-3′, and reverse primer: 5′- AGCTGACAGGTGGTGGCAAT-3′.

RNA sequencing

Tissue biopsies were collected by core needle biopsy on Day −6 (1 day before lymphodepletion) and on Day 11 after CAR T-cell infusion when adequate CAR T-cell expansion was detected, placed into RNA stabilization reagent (RNAlater; Qiagen), and frozen at −80°C. RNA was extracted using TRIzol and RNeasy MinElute Cleanup Kit (Qiagen). RNA purification, reverse transcription, library construction, and sequencing were performed according to the manufacturer's instructions (Illumina). Sequencing library was constructed using TruSeq RNA Samples Preparation Kit (Illumina). Qubit (Thermo Fisher Scientific) was used to quantify concentration of the resulting sequencing libraries, whereas the size distribution was analyzed using Agilent BioAnalyzer 2100 (Agilent). After library validation, clusters were generated by Illumina cBOT cluster generation system with HiSeq PE Cluster Kits (Illumina). Paired-end sequencing was performed using an Illumina HiSeq system following Illumina-provided protocols for 2 × 150 paired-end sequencing. The data are available under BioProject accession codes PRJNA531552 (https://www.ncbi.nlm.nih.gov/sra).

qRT-PCR

Total RNA was reversely transcribed using PrimeScript RT Reagent Kit (Takara) and qRT-PCR was performed by SYBR Green PCR master mix (Takara) according to the manufacture's protocol. All PCR reactions were performed in triplicate and the $2^{-\Delta\Delta}$Ct method was used to calculate the results. The sequence of PCR primers were listed in Supplementary Table S1.

IHC and immunofluorescence assay

IHC was performed on 5-μm paraffin sections with an indirect method (EnVison) using primary antibodies against CD3, CD19, CD20, CD68, CD163 (Dako, IR503, IR656, IR604, IR613, ZSGB-Bio, ZM-0428), and anti-rabbit- or anti-mouse-IgG as second antibodies (Dako; GV809, GV821). IHC was also performed using primary antibodies against EGFR (Santa Cruz Biotechnology; sc-120), Ki67 (Dako; M72400), and anti-mouse-IgG as second antibody. Immunofluorescence assay was performed on 4-μm frozen sections using primary antibodies against EGFR (Santa Cruz Biotechnology; sc-120), CD3 (Abcam; ab5690), CD68 (Abcam; ab125212), and Alexa Fluor-594-conjugated goat anti-mouse IgG H&L (Abcam; ab150120) and Alexa Fluor-488-conjugated goat anti-rabbit IgG H&L (Abcam; ab150077) as secondary antibodies, respectively. Nuclei were counterstained with DAPI. For absolute quantification, 5 randomly selected HPFs (×200 for IHC and ×600 for immunofluorescence assay) were analyzed in each section.

Macrophage differentiation

Human $CD14^+$ monocytes were isolated from PBMCs of healthy volunteers by using magnetic columns (Miltenyl Biotec; Catalog No. 130-042-401) following the manufacturer's instructions. $CD14^+$ monocytes were seeded at a cell density of 2.0 to 3.0×10^5 cells/mL in RPMI1640 medium with 2 mmol/L L-glutamine supplemented with 10% heat inactivated FBS, 100 U/mL penicillin, and 100 mg/mL streptomycin at 37°C in a humidified 5% CO_2 incubator. For M2 macrophage differentiation, cytokines CSF (R&D Systems; Catalog No. 216-MC-005), IL4 (R&D Systems; Catalog No. 204-IL-010), IL6 (R&D Systems; Catalog No. D6050), and IL13 (R&D Systems; Catalog No. 213-ILB-005) were used at a concentration of 20 ng/mL for each (15).

T-cell suppression assay

To determine the ability of M2 macrophages to suppress T-cell proliferation *in vitro*, carboxyfluorescein succinimidyl ester (CFSE; Thermo Fisher Scientific; Catalog No. 46410) stained T cells were stimulated for 3 days using Dynabeads human T-activator CD3/CD38 (Thermo Fisher Scientific; Catalog No. 11131D) and cultured in the absence or presence of M2 macrophages to T cells at 1:1 ratio. Cells were harvested, washed, and stained for surface markers and CFSE dilution was used as a measure of cell proliferation. Samples were acquired on a FACSFortessa (BD Bioscience) and data were analyzed using the FlowJo software 10.5.

Statistical analysis

The sample size estimation was based on the MTD. Dose escalation stopped when the safety evaluation of DL3 was accomplished, and approximately 10 patients were estimated. Regarding the ORR, another primary endpoint of concern, 10 patients provided 40% power to detect the difference between 65% and 40%, if we assumed the expected ORR of JWCAR029 was 65% (2-sided $\alpha = 0.05$). All data were tested for normal distribution (D'Agostino-Pearson omnibus normality test) before analyses. If the data were normal, a *t* test or 1-way ANOVA was used. For nonnormal data, nonparametric tests (Wilcoxon signed-rank test or Friedman test) were used (GraphPad Prism v7). All comparisons used a 2-sided α of 0.05 for significance testing.

Results

Patient characteristics

As shown in Fig. 1A, 15 patients were screened, and 10 patients were enrolled in this study, including 9 patients with DLBCL and 1 patient with marginal zone lymphoma. The reasons for 5 patients not enrolled in the study after screening included 3 patients not

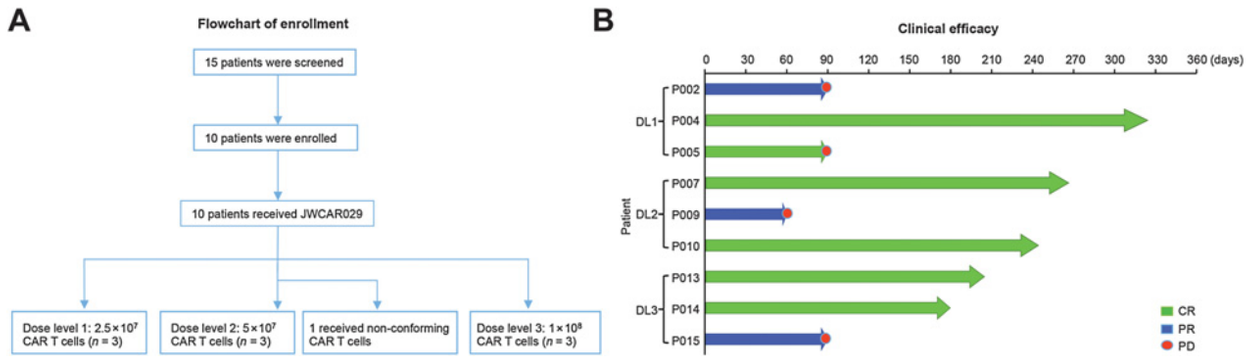

Figure 1.

Clinical enrollment and efficacy of JWCAR029 therapy. **A,** Study participant flow chart. **B,** Objective response rate among the 9 evaluable patients. DL1, dose level 1, DL2, dose level 2, DL3, dose level 3. CR, complete remission (green); PR, partial remission (blue); PD, progression disease (red). *X*-axis label indicates the days counted from treatment start.

meeting the criteria of relapsed or refractory B-NHL, 1 patient with inadequate pulmonary function, and 1 patient with persistent pancytopenia. Among all patients enrolled in the study, CAR T cells (JWCAR029) were manufactured and administered. Nine patients were allocated from DL1 to DL3 levels. The median time from leukapheresis to delivery of CAR T cells was 34.3 days. The dose and potency of CAR T cells were listed in Supplementary Table S2. One patient in the DL2 group received non-conforming CAR T cells (product that does not meet only one specification for certain predefined nonsafety-related attributes, and safety-related attributes all meet the specification. The exception release criteria for the nonsafety-related attribute of this patient was potency of CAR T cells) and was not included in the efficacy analysis.

Patient characteristics were summarized in Table 1. The median age was 47 years (range 32–59). All patients were CD19$^+$, had stage III or IV disease and were categorized into the intermediate-high and high-risk International Prognostic Index groups. The patients received a median of 4 prior lines of therapy (range 3–5). Seven patients with DLBCL were ineligible for autologous HSCT due to rapid tumor progression, and 1 patient with DLBCL relapsed at 2 months after autologous HSCT. Two patients received bridging chemotherapy after leukapheresis due to rapid tumor progression, followed by re-evaluation before CAR T-cell infusion as stable disease.

Table 1. Patient characteristics

Characteristics	*N* = 10
Age (years)	
Median (range)	47 (32–59)
Sex	
Male	8/10 (80%)
Female	2/10 (20%)
Pathologic diagnosis	
Diffuse large B-cell lymphoma	
Germinal center B-cell	2/10 (20%)
Non-germinal center B-cell	7/10 (70%)
Marginal zone B-cell lymphoma	1/10 (10%)
Ann Arbor	
I or II	0/10 (0%)
III or IV	10/10 (100%)
Extranodal lesions	
Yes	10/10 (100%)[a]
No	0/10 (0%)
Lactic dehydrogenase	
Normal	0/10 (0%)
Elevated	10/10 (100%)[b]
Performance status (ECOG)	
0	0/10 (0%)
1	10/10 (100%)
International Prognostic Index	
Intermediate (3)	9/10 (90%)
High risk (4–5)	1/10 (10%)
Prior lines of therapy	
3[c]	5/10 (50%)
4	4/10 (40%)
5	1/10 (10%)

Abbreviation: ECOG, Eastern Cooperative Oncology Group.
[a]Median (range): 3 (2–5).
[b]Median (range): 367 IU/L (260–656 IU/L); Normal: 98–192 IU/L.
[c]One patient relapsed after autologous stem-cell transplantation.

Overall activity

The date of data cut-off for the primary analysis was February 28, 2019. Among the 9 evaluable patients for efficacy, the median follow-up time was 6.5 (range 2.0–10.8) months. All patients achieved an objective response within 29 days after CAR T-cell infusion, with a CR rate of 66.7% (2 CR patients each in DL1, DL2, and DL3). Five patients were in continuous CR at 6 months after CAR T-cell infusion without receiving any further therapy including HSCT, except for 1 patient in DL1, who had tumor progression at 3 months and maintained stable disease upon ibrutinib treatment in combination with local radiotherapy. The 3 patients with partial remission (PR) showed partial metabolic response (14) at Day 29 (Supplementary Fig. S1) and disease progression occurred at 2 or 3 months (Fig. 1B). One PR patient received CD19 and CD22 CAR T infusion and remained alive without further treatment, whereas the other 2 PR patients died due to lymphoma progression.

Safety

The most common AEs of any grade were neutropenia (10/10, 100%), hypo-immunoglobulinemia (10/10, 100%), and pyrexia (8/10, 80%), with AEs of grade 3 or higher of neutropenia (10/10, 100%), anemia (3/10, 30%), thrombocytopenia (3/10, 30%), and hypofibrinogenemia (2/10, 20%). Grade 1 CRS occurred in all patients, with major symptoms such as fever (>38.6°C), fatigue, and muscle soreness (Supplementary Table S3). The median time to development of CRS was 6 days (range 3 to

11), and the median duration was 7 days (range 1–18). Grade 3 neurotoxicity occurred in one patient, who had ongoing grade 1 calculation defects (counting backward by serial 7s), and difficulty executing complex commands (handwriting). CRS and neurotoxicity were found to be self-limiting and reversible. Eight patients received tocilizumab (8 mg/kg), and 2 received glucocorticoids for the management of CRS, neurologic events, or both.

Pharmacokinetics

Serial blood samples were analyzed for CAR T-cell levels and serum biomarkers in the 9 evaluable patients for efficacy, as described previously (16). Using flow cytometry, CAR T-cell levels peaked in peripheral blood within 11 to 29 days after infusion and were detectable in 9 patients at 90 days after infusion. There was no significant difference in peak value and peak day of CAR T cells among different dose levels (Fig. 2A; Supplementary Fig. S2A). CAR T-cell persistence was confirmed by qRT-PCR (Fig. 2B). Among the 6 CR patients, CAR+ T cells were detected on Day 90 in 5 patients (Case 004, 005, 010, 013, and 014).

In terms of remission status on Day 29, the peak values of $CD3^+$ and $CD3^+CD8^+$ CAR T cells in the CR group were significantly higher than those of the PR group (Fig. 2C; Supplementary Fig. S2B). For the peak days, the 6 patients from CR group reached the peak of expansion on Day 8 to 15 (median Day 11), whereas the 3 patients from PR group on Day 15, 15, and 29, respectively. It should be pointed out that P015 reached the first peak at Day 11 (5×10^4 cell/mL), followed by the second peak at Day 29 (9.23×10^4 cell/mL). Patterns of serum biomarkers IL6, IL8, IL10, IL1β, IL2R, TNFα, CRP, and ferritin were similar (Fig. 2D), with no significant difference in the peak value or the peak day between the CR and PR group (Fig. 2E). Additionally, serum biomarker levels were not associated with the dose of CAR T cells (Supplementary Fig. S2C).

Microenvironment influence

To investigate the role of the tumor microenvironment on the clinical response, we performed RNA sequencing on tumor samples of 8 patients with DLBCL before CAR T-cell treatment and identified the transcriptomic signatures that were differentially enriched in the CR and PR patients. We first compared the immunosuppressive gene expression of the tumor microenvironment. The CR group displayed decreased levels of chemokines that negatively regulate the recruitment of tumor-associated macrophages (TAM) (*CCL2*, *CXCL8*; refs. 17, 18), Tregs, and MDSCs (*CXCL12*, *CCL3*, *CCL4*, *CCL5*; refs. 19–21) to the tumor microenvironment. Instead, overexpression of *CXCL9*, *CXCL10*, *CXCL11*, and *CXCL16* in the PR group indicated the presence of tumor-associated dendritic cells that also possess immunosuppressive functions (22). Meanwhile, immunosuppressive cytokines (*IL10*, *TGF-β1*), as well as MDSCs (*CD33*, *CD14*) and tumor-associated fibroblasts (*FAP*, *TNC*, *CSPG4*, *PDGFRA*, *S100A4*, *ASPN*, *STC1*, *ITGAM*) were higher in the PR group than in the CR group (Fig. 3A), suggesting that the pretreatment immunosuppressive status of the tumor microenvironment may impacts the CAR T therapy response.

To better understand the potential mechanism of immune suppression, we next provided an analysis to identify immunosuppressive components of the tumor microenvironment. As

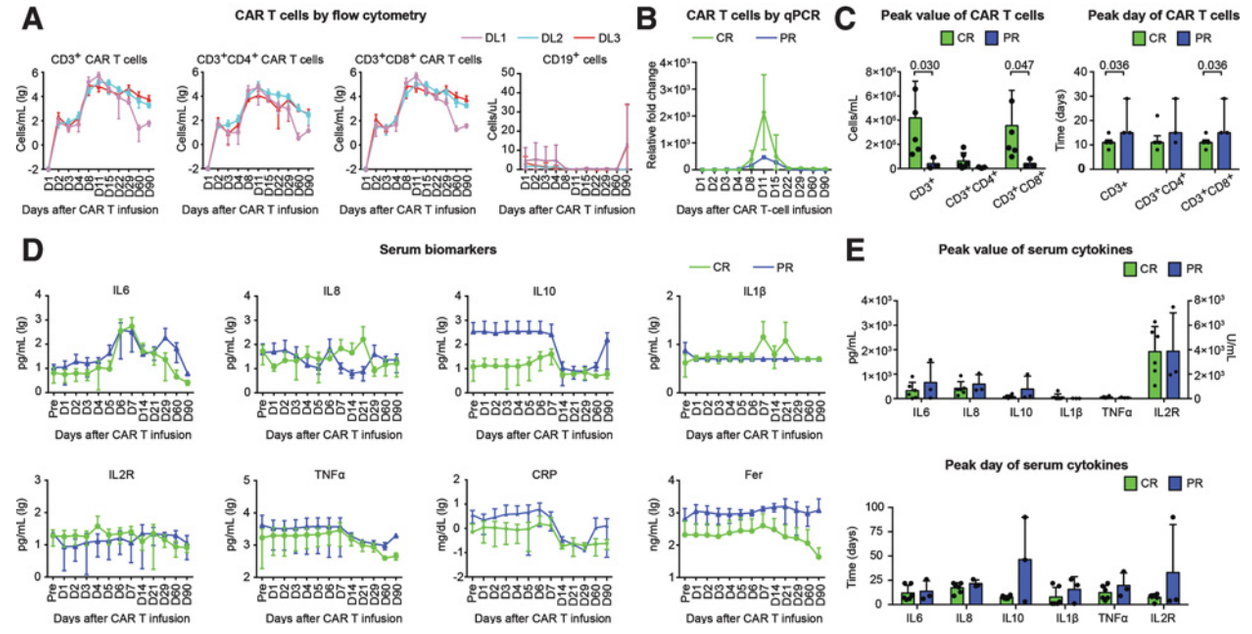

Figure 2.

Kinetics of peripheral blood CAR-T cells and serum biomarkers. **A,** CAR T-cell and B-cell count (mean ± SD) change over time from peripheral blood in DL1 (purple), DL2 (blue), and DL3 (red). **B,** Relative fold change of EGFRt+ CAR T cells detected by qRT-PCR over time from peripheral blood in the CR (green line) and PR group (blue line). Limit of detection of PCR assay is 0.001%. **C,** Bar plots showing the comparison of the peak value (mean ± SD) and the peak day (median ± IQR) of CAR T cells in the CR (green) and PR group (blue). **D,** The concentration of serum biomarkers (mean ± SD) change over time in the CR (green) and PR group (blue). **E,** Bar plots showing the comparison of the peak value (mean ± SD) and the peak day (median ± IQR) of serum cytokines in the CR (green) and PR group (blue). Student *t* test, one-way ANOVA, Wilcoxon signed-rank test or Friedman test was used, as appropriate. IQR, interquartile range.

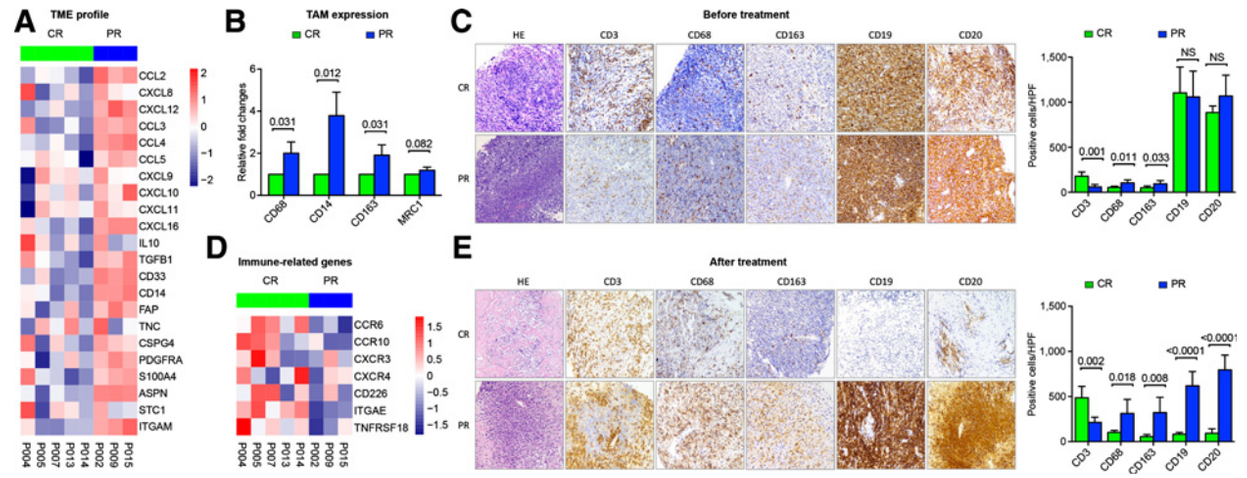

Figure 3.

Correlation of tumor microenvironment feature with clinical outcome. **A,** Heat maps showing normalized expression of genes associated with the immunosuppressive tumor microenvironment. Samples were annotated by CR and PR. **B,** qRT-PCR showing gene expression of tumor-associated macrophages (TAM) in the CR and PR groups. **C,** HE and IHC straining of CD3, CD68, CD163, CD19, and CD20 expression in tumor samples collected from the CR and PR patients before treatment. The cells were counted from 5 randomly selected visions and subjected for statistical analysis. **D,** Heat maps showing normalized expression of genes associated with immune-related chemokine receptors and adhesion molecules. **E,** HE and IHC staining of CD3, CD68, CD163, CD19, and CD20 expression in tumor samples collected from the CR and PR patients after treatment. The cells were counted from 5 randomly selected visions and subjected for statistical analysis. NS, not significant.

expected, the expression of CD68, CD14, and CD163, which are expressed on TAMs, were significantly increased in the PR group by qRT-PCR (Fig. 3B). It is well established that TAMs with M2 phenotype may inhibit T-cell function and proliferation (23). As revealed by immunohistochemistry, the PR group presented with increased $CD68^+$ and $CD163^+$ cells, the later representing M2 macrophages, and decreased $CD3^+$ cells, as compared with the CR group. Similar distribution of $CD19^+$ and $CD20^+$ cells was observed between 2 groups, indicating that CD20 expression did not compensate loss of CD19 expression (Fig. 3C). Thus, tumor microenvironment composition was in agreement with chemokine/cytokine profiles noted by transcriptomic signatures, and could affect antitumor T cells and CAR T-cell efficacy.

Interestingly, in terms of remission status, increased expression of immune-related chemokine receptors (*CCR6*, *CCR10*, *CXCR3*, *CXCR4*) and adhesion molecules (*CD226*, *ITGAE*, *TNFRSF18*) were observed in the CR group (Fig. 3D). Moreover, expression levels of activating and inhibitory markers were assessed by qRT-PCR. The CR group highly expressed activating markers including *ICOS*, *B3GAT1* (CD57), *TBX21* (T-bet), *TNFRSF9* (4-1BB), as well as inhibitory markers *LAG3*, *CTLA4*, *CD160* that are also upregulated on activated T cells (Supplementary Fig. S3A and S3B), suggesting that T-cell activation was related to clinical response. Together, the tumor microenvironment was conducive to T cells for activation in CR patients, which were "hot" tumors. In contrast, "cold" tumors of the PR patients had a distinct immunosuppressive tumor microenvironment not favorable for tumor-infiltrating lymphocytes.

We further performed IHC staining of tissue samples collected on Day 11 after CAR T treatment to verify that TAMs mediate the immunosuppressive microenvironment and affect CAR T-cell proliferation. In the CR patients, $CD3^+$ T cells were distributed inside the tumor, and there were fewer $CD68^+$, $CD163^+$, and $CD19^+/CD20^+$ cells. However, in the PR patients, $CD3^+$ T cells were excluded from tumor cells, where $CD68^+$ and $CD163^+$ cells were abundant (Fig. 3E). These findings supported the notion that TAMs could serve as a negative predictor for CAR T-cell efficacy. Meanwhile, to reveal the identity of tumor-infiltrating T cells after CAR T-cell infusion, we performed the confocal study using anti-EGFR antibody and anti-CD3 antibody to distinguish exogenous and endogenous T cells. Both endogenous $CD3^+$ and exogenous $EGFR^+$ T cells were enriched in the CR patients after treatment, but rarely observed in the PR patients (Fig. 4A). Correspondingly, fewer $CD68^+$ TAMs were seen in the CR patients than in the PR patients (Fig. 4B).

To mimick the negative regulation of TAMs with M2 phenotype macrophages on tumor-infiltrating T cells *in vitro*, we isolated human $CD14^+$ monocytes from healthy donors and differentiated them into M2 macrophages, which have the same phenotype of TAMs as reported previously (24). M2 macrophages were cocultured with T cells at 1:1 ratio. M2 macrophages significantly suppressed the percentage of proliferation in both autologous $CD4^+$ T (with M2 macrophages, median 30.0, range 23.0–36.8, $n = 4$; without M2 macrophages, median 69.0, range 67.1–77.0, $n = 4$) and $CD8^+$ T (with M2 macrophages, median 40.5, range 32.0–48.8, $n = 4$; without M2 macrophages, median 80.5, range 73.0–88.0, $n = 4$) cells (Fig. 4C). The PR patients also presented with significantly decreased double $EGFR^+Ki67^+$ cells, as compared with the CR patients (Supplementary Fig. S4), further indicating that T-cell proliferation was suppressed by tumor microenvironment of the PR group after CAR T treatment.

Discussion

CAR T cells specifically targeting tumor immunity have shown promising efficacy in the treatment of various hematologic malignancies, particularly B-NHL. To date, a number of studies aim at dissecting factors that impact the clinical response and have

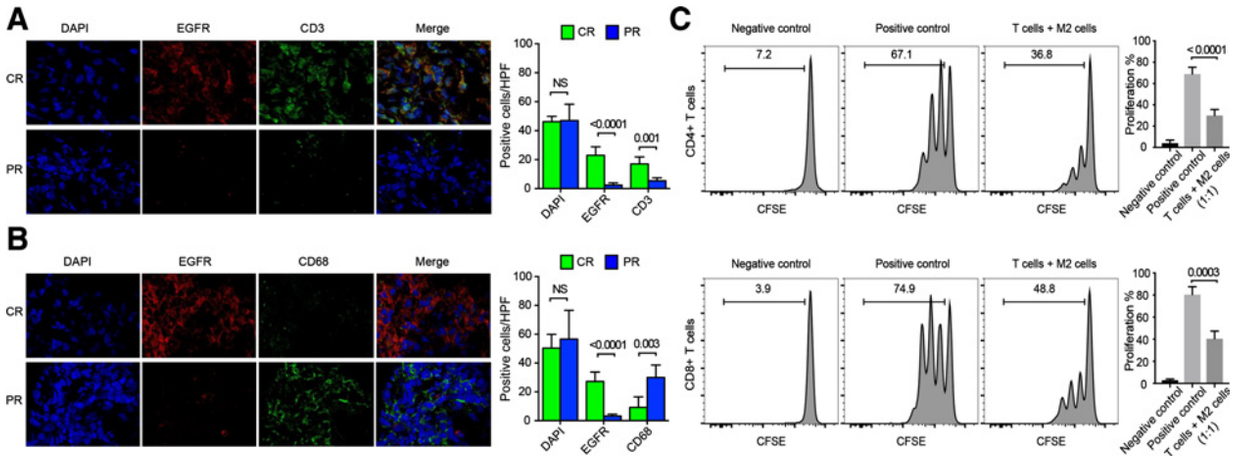

Figure 4.

Correlation of TAMs with infiltrating T cells. **A,** Confocal analysis of CAR$^+$ T cells (EGFR$^+$) and T cells (CD3$^+$) in tumor samples collected from the CR and PR patients after treatment. The cells were counted from 5 randomly selected visions and subjected for statistical analysis. **B,** Confocal analysis of the CAR$^+$ T cells (EGFR$^+$) and TAMs (CD68$^+$) in tumor samples collected from the CR and PR patients after treatment. The cells were counted from 5 randomly selected visions and subjected for statistical analysis. Bar plots showing the comparison of frequency of CAR T cells, T cells, and TAMs in the CR and PR group. **C,** Proliferation of CD4$^+$ (top) and CD8$^+$ (bottom) T cells in response to M2 macrophages. The negative control was T cells without stimulation, positive control was T cells with CD3 and CD28 stimulation, or T cells coculture with M2 macrophages in CD3 and CD28 stimulation condition for 72 hours. The results are representative of 4 independent experiments using cells derived from an individual donor. Bar plots showing the statistics analysis of proliferation in the conditions described earlier for 4 independent experiments (median with interquartile range). NS, not significant.

identified expansion of CAR T cells as major determinants of response to CAR T therapy. In this phase I, first-in human study of JWCAR029, the CR rate was 66.7%, which is consistent with results from the ZUMA-1, JULIET, and TRANSCEND studies. Notably, the dose escalation allowed us to find the patients achieving CR with low doses of CAR T cells, indicative of an alternative mechanism relating to the clinical response of CAR T therapy.

Previous studies revealed the effect of immune-related factors on the clinical outcome of CAR T therapy. In B-NHL, elevated serum IL15 level was associated with high CAR T-cell peak levels in peripheral blood and with remission status (25). Other serum markers associated with durable response include CXCL10, IL8, IL10, MCP-1, MIP-1β, and TNFα (26). Enrichment of the less-differentiated T subset of infused CAR T cells induced CR more frequently in patients with chronic lymphocytic leukemia (27). To our knowledge, this is the first study to investigate the potential impact of the tumor microenvironment on the CAR T-cell efficacy. Here, we observed distinct gene expression signatures between patients with or without CR by analyzing RNA sequencing data generated from tumor samples and showed that tumor microenvironment may create an immunosuppressive milieu to inhibit CAR T-cell proliferation in tumor sites, which are unfavorable for antitumor activity. Several factors negatively influencing tumor-infiltrating T-cell function have already been described. Dysfunction of the T-cell response is mediated by the secretion of anti-inflammatory cytokines, such as IL10 and TGFβ, production of chemokines that promote tumor progression through recruitment of Treg and MDSC cells (28–30), as well as involvement of TAMs, tumor-associated dendritic cells and fibroblasts (9). This phenomenon can explain why CAR T cells are unable to attack the tumors and how the lack of immune cells occurs in the tumor microenvironment and leads to treatment failure.

Furthermore, we reasoned that the composition of the tumor microenvironment modulated the *in situ* persistence of CAR T cells within the tumors. As we know, TAMs play an important role in the immune response (31). The quantities and polarization states of TAMs have been shown to contribute to the emergence of an immunosuppressive microenvironment and suppression of the T-cell response. M2 macrophages generally produce high levels of IL10 and TGFβ. Interestingly, we found that the levels of M2 macrophages, identified through CD68 and CD163 expression, were significantly enriched within tumor samples of patients without CR. Meanwhile, TAMs may create a hostile microenvironment, mitigate the CAR T-cell response, and serve as a predictive marker of treatment failure. Strategies to deplete TAMs could improve the clinical efficacy of CAR T therapy in patients with B-NHL, which also drive decision making regarding CAR T therapy. For patients with primary refractory disease or early relapse that are more likely to be sensitive, CAR T therapy may be applied in earlier-line settings, or with reduced doses to avoid severe toxicities.

T-cell activation and proliferation are induced by activating markers. In terms of remission status, costimulatory molecules (ICOS and 4-1BB) were significantly higher in the CR patients. In addition, LAG3 and CTLA-4 are not only expressed in exhausted T cells, but also on activating and proliferating T cells (32). This can explain why increased levels of these markers were also observed in the CR group. The tumor microenvironment in the CR patients is thought to effectively attract CAR T cells to tumor sites and favors T-cell activation and proliferation through the production of appropriate chemokines. Immune checkpoint inhibitors can be used in combination with CAR T cells to enhance the antitumor efficacy. The immunosuppressive tumor microenvironment may be targeted by immunomodulatory agents, tipping the balance in favor of T-cell activation (29, 31, 33). This mechanism is helpful

for identifying which targetable immune pathways may be optimal for specific patient populations.

This study still has some limitations. For example, the sample size in our study was very small with only 10 patients included in the phase I, dose-escalation study evaluating JWCAR029 safety in refractory B-NHL. We may not draw any definite conclusion based on the limited sample size. However, the potential influence of the tumor microenvironment on clinical efficacy gives a fruitful clue for future studies to patient selection of CAR T therapy. Moreover, because bulk RNA sequencing was performed, further biomarker analysis should be applied using single cell sequencing technique to a given cell population.

In conclusion, the composition of the tumor microenvironment is closely associated with the clinical response to CAR T therapy. Modulation of the tumor microenvironment through various strategies targeting TAMs and other immunosuppressive factors may have the potential for augmenting efficacy and attaining a more durable remission of CAR T therapy.

Disclosure of Potential Conflicts of Interest

W. Wang is an employee/paid consultant for Simcere Pharmaceutical Group. M. Hao and S. Yang are employees/paid consultants for JW Therapeutics. J. Li is an employee/paid consultant for and holds ownership interest in JW Therapeutics. No potential conflicts of interest were disclosed by the other authors.

Authors' Contributions

Conception and design: W.-L. Zhao
Development of methodology: W. Wang
Acquisition of data (provided animals, acquired and managed patients, provided facilities, etc.): Z.-X. Yan, L. Li, M.-C. Zhang
Analysis and interpretation of data (e.g., statistical analysis, biostatistics, computational analysis): Z.-X. Yan, L. Li, B.-S. OuYang, P.-P. Xu, M. Hao
Writing, review, and/or revision of the manuscript: Z.-X. Yan, L. Li, W. Wang, P.-P. Xu, M. Muftuoglu, W.-L. Zhao
Administrative, technical, or material support (i.e., reporting or organizing data, constructing databases): L. Wang, W. Wu, S. Yang, L. Li
Other (patient enrollment and management): S. Cheng, S. Yang, Z. Zheng

Acknowledgments

This study was supported, in part, by research funding from the National Natural Science Foundation of China (81520108003, 81830007, 81600155, and 81670716), National Key Research and Development Program of China (2016YFC0902800), Chang Jiang Scholars Program, Shanghai Commission of Science and Technology (16JC1405800), Shanghai Rising-Star Program (19QA145600), Municipal Human Resources Development Program for Outstanding Young Talents in Medical and Health Sciences in Shanghai (2017YQ075), Shanghai Municipal Education Commission Gaofeng Clinical Medicine Grant Support (20152206 and 20152208), Clinical Research Plan of SHDC (16CR2017A), multicenter clinical research project by Shanghai Jiao Tong University School of Medicine (DLY201601), Collaborative Innovation Center of Systems Biomedicine and Samuel Waxman Cancer Research Foundation.

The costs of publication of this article were defrayed in part by the payment of page charges. This article must therefore be hereby marked *advertisement* in accordance with 18 U.S.C. Section 1734 solely to indicate this fact.

Received January 9, 2019; revised April 16, 2019; accepted August 15, 2019; published first August 23, 2019.

References

1. Crump M, Neelapu SS, Farooq U, Van Den Neste E, Kuruvilla J, Westin J, et al. Outcomes in refractory diffuse large B-cell lymphoma: results from the international SCHOLAR-1 study. Blood 2017;130:1800–8.
2. Neelapu SS, Locke FL, Bartlett NL, Lekakis LJ, Miklos DB, Jacobson CA, et al. Axicabtagene ciloleucel CAR T-cell therapy in refractory large B-cell lymphoma. N Engl J Med 2017;377:2531–44.
3. Schuster SJ, Bishop MR, Tam CS, Waller EK, Borchmann P, McGuirk JP, et al. Tisagenlecleucel in adult relapsed or refractory diffuse large B-cell lymphoma. N Engl J Med 2019;380:45–56.
4. Abramson JS, Palomba ML, Gordon LI, Lunning MA, Arnason JE, Wang M, et al. High durable CR rates in relapsed/refractory (R/R) aggressive B-NHL treated with the CD19-directed CAR T cell product JCAR017 (TRANSCEND NHL 001): defined composition allows for dose-finding and definition of pivotal cohort [ASH abstract 581]. Blood. 2017;130(Suppl 1):581.
5. Orlando EJ, Han X, Tribouley C, Wood PA, Leary RJ, Riester M, et al. Genetic mechanisms of target antigen loss in CAR19 therapy of acute lymphoblastic leukemia. Nat Med 2018;24:1504–6.
6. Ruella M, Xu J, Barrett DM, Fraietta JA, Reich TJ, Ambrose DE, et al. Induction of resistance to chimeric antigen receptor T cell therapy by transduction of a single leukemic B cell. Nat Med 2018;24:1499–503.
7. Sotillo E, Barrett DM, Black KL, Bagashev A, Oldridge D, Wu G, et al. Convergence of acquired mutations and alternative splicing of CD19 enables resistance to CART-19 immunotherapy. Cancer Discov 2015;5:1282–95.
8. Craddock JA, Lu A, Bear A, Pule M, Brenner MK, Rooney CM, et al. Enhanced tumor trafficking of GD2 chimeric antigen receptor T cells by expression of the chemokine receptor CCR2b. J Immunother 2010;33:780–8.
9. Shah NN, Fry TJ. Mechanisms of resistance to CAR T cell therapy. Nat Rev Clin Oncol 2019;6:372–85.
10. Mantovani A, Longo DL. Macrophage checkpoint blockade in cancer - back to the future. N Engl J Med 2018;379:1777–9.
11. Van Heertum RL, Scarimbolo R, Wolodzko JG, Klencke B, Messmann R, Tunc F, et al. Lugano 2014 criteria for assessing FDG-PET/CT in lymphoma: an operational approach for clinical trials. Drug Des Devel Ther 2017;11:1719–28.
12. Li DH, Whitmore JB, Guo W, Ji Y. Toxicity and efficacy probability interval design for phase I adoptive cell therapy dose-finding clinical trials. Clin Cancer Res 2017;23:13–20.
13. Lee DW, Gardner R, Porter DL, Louis CU, Ahmed N, Jensen M, et al. Current concepts in the diagnosis and management of cytokine release syndrome. Blood 2014;124:188–95.
14. Cheson BD, Fisher RI, Barrington SF, Cavalli F, Schwartz LH, Zucca E, et al. Recommendations for initial evaluation, staging, and response assessment of Hodgkin and non-Hodgkin lymphoma: the Lugano classification. J Clin Oncol 2014;32:3059–68.
15. Zarif JC, Hernandez JR, Verdone JE, Campbell SP, Drake CG, Pienta KJ. A phased strategy to differentiate human CD14+monocytes into classically and alternatively activated macrophages and dendritic cells. BioTechniques 2016;61:33–41.
16. Turtle CJ, Hanafi LA, Berger C, Gooley TA, Cherian S, Hudecek M, et al. CD19 CAR-T cells of defined CD4+:CD8+ composition in adult B cell ALL patients. J Clin Invest 2016;126:2123–38.
17. Fridlender ZG, Buchlis G, Kapoor V, Cheng G, Sun J, Singhal S, et al. CCL2 blockade augments cancer immunotherapy. Cancer Res 2010;70:109–18.
18. Fang W, Ye L, Shen L, Cai J, Huang F, Wei Q, et al. Tumor-associated macrophages promote the metastatic potential of thyroid papillary cancer by releasing CXCL8. Carcinogenesis 2014;35:1780–7.
19. Muthuswamy R, Corman JM, Dahl K, Chatta GS, Kalinski P. Functional reprogramming of human prostate cancer to promote local attraction of effector CD8(+) T cells. Prostate 2016;76:1095–105.
20. Schlecker E, Stojanovic A, Eisen C, Quack C, Falk CS, Umansky V, et al. Tumor-infiltrating monocytic myeloid-derived suppressor cells mediate CCR5-dependent recruitment of regulatory T cells favoring tumor growth. J Immunol 2012;189:5602–11.
21. Patterson SJ, Pesenacker AM, Wang AY, Gillies J, Mojibian M, Morishita K, et al. T regulatory cell chemokine production mediates pathogenic T cell attraction and suppression. J Clin Invest 2016;126:1039–51.

22. Tran Janco JM, Lamichhane P, Karyampudi L, Knutson KL. Tumor-infiltrating dendritic cells in cancer pathogenesis. J Immunol 2015;194: 2985–91.
23. Yang L, Zhang Y. Tumor-associated macrophages: from basic research to clinical application. J Hematol Oncol 2017;10:58.
24. Mantovani A, Allavena P, Sica A, Balkwill F. Cancer-related inflammation. Nature 2008;454:436–44.
25. Rossi J, Paczkowski P, Shen YW, Morse K, Flynn B, Kaiser A, et al. Preinfusion polyfunctional anti-CD19 chimeric antigen receptor T cells are associated with clinical outcomes in NHL. Blood 2018;132: 804–14.
26. Siddiqi T, Abramson JS, Li D, Brown W, Devries T, Dave K, et al. Patient characteristics and pre-infusion biomarkers of inflammation correlate with clinical outcomes after treatment with the defined composition, CD19-targeted CAR T cell product, JCAR017. [ASH abstract 581]. Blood 2017; 130:193.
27. Fraietta JA, Lacey SF, Orlando EJ, Pruteanu-Malinici I, Gohil M, Lundh S, et al. Determinants of response and resistance to CD19 chimeric antigen receptor (CAR) T cell therapy of chronic lymphocytic leukemia. Nat Med 2018;24:563–71.
28. Seo N, Hayakawa S, Takigawa M, Tokura Y. Interleukin-10 expressed at early tumour sites induces subsequent generation of CD4(+) T-regulatory cells and systemic collapse of antitumour immunity. Immunology 2001; 103:449–57.
29. Ruffell B, Chang-Strachan D, Chan V, Rosenbusch A, Ho CM, Pryer N, et al. Macrophage IL-10 blocks CD8+ T cell-dependent responses to chemotherapy by suppressing IL-12 expression in intratumoral dendritic cells. Cancer Cell 2014;26:623–37.
30. van der Woude LL, Gorris MAJ, Halilovic A, Figdor CG, de Vries IJM. Migrating into the tumor: a roadmap for T cells. Trends Cancer 2017;3: 797–808.
31. Steidl C, Lee T, Shah SP, Farinha P, Han G, Nayar T, et al. Tumor-associated macrophages and survival in classic Hodgkin's lymphoma. N Engl J Med 2010;362:875–85.
32. Wei SC, Duffy CR, Allison JP. Fundamental mechanisms of immune checkpoint blockade therapy. Cancer Discov 2018;8:1069–86.
33. Wu X, Schulte BC, Zhou Y, Haribhai D, Mackinnon AC, Plaza JA, et al. Depletion of M2-like tumor-associated macrophages delays cutaneous T-cell lymphoma development in vivo. J Invest Dermatol 2014;134: 2814–22.